# Intensity of the Vaccine-Elicited Immune Response Determines Tumor Clearance

Ainhoa Perez-Diez,* Paul J. Spiess,* Nicholas P. Restifo,* Polly Matzinger,† and
Francesco M. Marincola[1]*‡

Tumor Ag-specific vaccines used for cancer immunotherapy can generate specific CD8 responses detectable in PBMCs and in tumor-infiltrating lymphocytes. However, human studies have shown that detection of a systemic vaccine-induced response does not necessarily correlate with the occasional instances of tumor rejection. Because this discrepancy might partially be attributable to the genetic heterogeneity of human cancers, as well as to the immunosuppressive effects of previous treatments, we turned to a mouse model in which these variables could be controlled to determine whether a relationship exists between the strength of vaccine-induced immune responses and tumor rejection. We challenged mice with the β-galactosidase (β-gal)-expressing tumor cells, C25.F6, vaccinated them with β-gal-carrying viral vectors, and used quantitative RT-PCR to measure the vaccine-induced immune response of splenocytes directly ex vivo. We found that the strength of the response increased with increasing doses of β-gal-carrying vector and/or upon boosting with a heterologous β-gal-carrying virus. Most importantly, we found that the strength of the detected immune response against this foreign Ag strongly correlated with reduction in the number of lung metastases. The results from this mouse model have major implications for the implementation of tumor vaccines in humans. *The Journal of Immunology,* 2002, 168: 338–347.

Following the identification of tumor-associated Ags recognized by T cells (1–3) tumor Ag-specific cancer vaccines have been developed which, in some cases, have succeeded in generating anti-tumor immune responses detectable in PBMC by in vitro (4) and, more recently, ex vivo assays (5, 6). However, the generation of detectable Ag-specific CD8 responses only occasionally results in clinical tumor rejection (7–9). Several possibilities might explain these conflicting results: 1) Ag-specific CD8$^+$ T cells might be unable to leave the peripheral circulation and reach the tumor; 2) vaccine-elicited CD8$^+$ T cells might be functionally inactive; and 3) the immune responses elicited by the vaccine might be qualitatively inappropriate or quantitatively insufficient. The first two possibilities are unlikely, as functional vaccine-induced CD8$^+$ T cell responses have been documented at the tumor site (10–13). The third is more likely. Although tumor-reactive T cells effectively producing Th type-1 cytokines have been documented in vaccine-naive patients with cancer (14) as well as in response to vaccination (15), the immune responses to vaccination might be below a required quantitative threshold or they might be of the wrong effector class for immune rejection of tumors. This obvious question has remained unanswered largely due to a lack of direct methods able to accurately assess the magnitude of functional immune responses ex vivo. In fact, methods for the monitoring of vaccine-induced immune responses have generally aimed at enhancing sensitivity by amplifying the cognate CTL populations using in vitro sensitization and/or expansion

steps (16–18). Recent work from our group has shown that direct ex vivo methods for enumeration of immune responses usually detect vaccine-induced immunity less frequently than methods that include in vitro expansion with arbitrary doses of epitope and immune-proliferative stimuli such as IL-2 (12, 19). Thus, it is likely that the immune response to vaccines in vivo may be weaker than in vitro sensitization assays had previously suggested. Therefore, one might expect that ex vivo measures of the strength of vaccine-induced immunity might correlate more closely with tumor rejection than previous in vitro measures. However, in preliminary clinical trials we found that this was not the case and that ex vivo measures of vaccine-induced immunity also lacked predictive value with regard to the desired clinical outcome (19). It is also possible that the lack of clinical response despite cellular immune response may reflect escape of tumor cells from immune recognition. We postulated that further efforts to measure a correlation between the magnitude of immune response to vaccination and the clinical outcome might be hampered in human subjects by the extreme variability of late-term cancer patients, the heterogeneity of their tumors, and the immunosuppressive effects of previous treatments.

Thus, to determine, in principle, whether tumor rejection depends on the strength of a vaccine-induced response as opposed to its mere presence, we developed a mouse model in which the recipients are immunologically functional and where other factors can be standardized by homogeneity of the reagents and procedures adopted. In this simplified model, we assessed whether the strength of the immune response to an Ag expressed by tumor cells could be used as a marker to predict the clinical outcome. By implanting known numbers of a stable tumor clone into a set of inbred animals, heterogeneity due to the genetic instability of neoplasia, or to the variability of the host, was minimized. We chose a β-galactosidase (β-gal)$^2$-transduced tumor, in which two

---

[1] Address correspondence and reprint requests to Dr. Francesco M. Marincola, Surgery Branch, National Cancer Institute, Room 2B42, Building 10, 10 Center Drive, MSC 1502, Bethesda, MD 20892-1502. E-mail address: marincola@nih.gov

[2] Abbreviations used in this paper: β-gal, β-galactosidase; qRT-PCR, quantitative RT-PCR; FDG, fluorescein di-β-galactopyranoside; βVV, β-gal expressing recombinant vaccinia virus; βFPV, β-gal expressing recombinant fowl pox virus; cVV, control recombinant vaccinia virus; cFPV, control recombinant fowl pox virus; Ct, cycle threshold; Flu, peptide from influenza.

heterologous fowl pox-based viral vectors carrying the $\beta$-gal Ag were able, in previous studies, to cure lung metastases in 80% of mice (20). In this model, specific CD8$^+$ T cells that recognize an H-2L$^d$ restricted epitope (TPHPARIGL) appear essential for tumor rejection. We then developed various sets of primers and probes suitable for real-time quantitative RT-PCR (qRT-PCR)-based direct quantification of $\beta$-gal-specific CD8$^+$ T responses in splenocytes of vaccinated mice. Using this model, we observed that the strength of the response, as measured directly ex vivo, does indeed correlate with tumor rejection.

## Materials and Methods
### Mice

Female BALB/c mice, 6–10 wk old, were obtained from the Animal Production Colonies, National Cancer Institute-Frederick Cancer Research and Development Center, National Institutes of Health (Frederick, MD). The mice received care in accordance with the guidelines set forth by the Animal Research Advisory Committee of the National Institutes of Health. The National Institutes of Health is an American Association for the Accreditation of Laboratory Animal Care-accredited institution.

### Tumor cell lines

CT26 is a colon carcinoma of BALB/c origin. CT26.CL25 is a $\beta$-gal-expressing cell line previously described (21). C25.F6 (F6) is a stable clone expressing high levels of $\beta$-gal obtained as follows. High expressing $\beta$-gal CT26.CL25 cells were sorted and cultured at 1 cell/well without G418. After a first screening, we again sorted the highest expressing $\beta$-gal cells from the positive clones and cultured them in the absence of G418 to assess genetic stability. After a second screening, F6 was selected among other clones because of its stable expression of high levels of $\beta$-gal. Cell lines were maintained in complete medium consisting of RPMI 1640, 10% heat-inactivated FCS (Biofluids, Rockville, MD), 0.03% L-glutamine, 100 $\mu$g/ml streptomycin, 100 U/ml penicillin, and 50 $\mu$g/ml gentamicin sulfate (National Institutes of Health Media Center).

### Detection and sorting of $\beta$-gal-expressing cells by FACS

To detect and sort $\beta$-gal-expressing tumor cells, we used the fluorescein di-$\beta$-galactopyranoside (FDG) assay procedure (22).

### Peptides

The peptide TPHPARIGL, a $\beta$-gal epitope presented by H-2L$^d$ Ags (aa 876–884), was synthesized by Macromolecular Resources (Colorado State University, Fort Collins, CO) to a purity of >95%. The influenza nucleoprotein peptide (QL9) QLSPFPFDL, also presented by H-2L$^d$, was synthesized using standard F-moc (N-a-9-fluorenylmethoxycarbonyl) chemistry.

### Recombinant viruses

The $\beta$-gal-expressing recombinant vaccinia ($\beta$VV) and recombinant fowl pox ($\beta$FPV) viruses have been previously described (20). As control vaccination, we used the same recombinant viruses, but lacking the LacZ gene (cVV and cFPV, respectively).

### In vivo treatment of lung nodules

BALB/c mice were challenged i.v. with 10$^5$ F6 tumor cells to establish lung nodules. Three days later, the mice were primed with either no immunogen (untreated mice), 10$^7$ PFU of cFPV, or serial 10-fold dilutions of $\beta$FPV administered i.v. or i.p. as described in each experiment. Fifteen days after tumor inoculation, each group was boosted with the same amount of either no immunogen, cVV, or $\beta$VV. Seven days after the second vaccination, mice were sacrificed and metastatic lung nodules were enumerated in a randomized manner. Splenocytes from randomly chosen individual mice from each experimental group were analyzed for ex vivo quantification of anti-$\beta$-gal-specific reactivity by qRT-PCR.

### Ex vivo quantification of anti-$\beta$-gal-specific reactivity by real-time qRT-PCR

Splenocytes from untreated or vaccinated mice (5 $\times$ 10$^5$ cells) were plated in 100 $\mu$l of medium in U-bottom 96-well plates and incubated overnight at 37°C in 5% CO$_2$. Peptide (1 $\mu$M) or tumor cells (1 $\times$ 10$^5$) were then added in a total volume of 200 $\mu$l/well and incubated at 37°C in 5% CO$_2$

for 2 h. The cells were then harvested for RNA isolation with RNeasy mini kits (Qiagen, Santa Clarita, CA) and cDNA transcription, with cDNA transcription reagents (PerkinElmer, Foster City, CA) using random hexamers. qRT-PCR was performed for IL-2, IL-4, IL-10, TNF-$\alpha$, and IFN-$\gamma$ mRNA expression and normalized to copies of CD8 mRNA, e.g., the number of copies of cytokine mRNA/the number of copies of CD8 mRNA.

### Real-time qRT-PCR

Quantification of gene expression was performed using the ABI prism 7700 sequence detection system (PerkinElmer) as previously described (12). TaqMan probes were labeled at the 5′ end with the reporter dye molecule 6-carboxyfluorescein and at the 3′ end with the quencher dye molecule 6-carboxytetramethylrhodamine. RT-PCR of cDNA specimens and cDNA standards were conducted in a total volume of 25 $\mu$l with 2$\times$ TaqMan master mix (PerkinElmer) and primers and probes at optimized concentrations (200 and 100 nM, respectively). Real-time monitoring of fluorescence emission from cleavage of sequence-specific probes by Taq polymerase allowed definition of the cycle threshold (Ct, the cycle at which fluorescence exceeds 10 times the SD above the mean of the background) during the exponential phase of amplification (23). Standard curves were generated for each gene quantified and the reagents were found to have excellent PCR amplification efficiency as determined by the slope of the standard curves. Linear regression analysis showed that all standard curves had $R \geq 0.99$. Standard curve extrapolation of a copy number was performed for the gene of interest as well as for the endogenous reference gene (CD8) for each sample. Normalization of samples was performed by dividing the copies of the gene of interest by the copies of the CD8 reference gene. All PCR assays were performed in duplicate and their Ct values (SD < 0.5) are reported as the average.

### Statistical analysis

The mean and the SD of the number of lung metastases and the ratio of IFN-$\gamma$ for each group of mice were calculated. Statistical significance of the observed differences was assessed by two-tailed Student's t test.

## Results
### The measurement system: ex vivo quantification of cytokine mRNA production by qRT-PCR

To develop a method for the quantitative ex vivo measurement of $\beta$-gal-specific responses generated in mice, we designed primers and probes for mouse IL-2, IL-4, IL-10, TNF-$\alpha$, IFN-$\gamma$, and CD8 genes (Fig. 1a) to be used in qRT-PCR. Fig. 1b shows a sample of the plots for 10-fold dilutions of the standard for TNF-$\alpha$. Samples containing high concentrations of cDNA (large circles) reach the threshold cycle earlier than samples with low amounts of cDNA (smaller circles). We designated Ct, on the linear portion of the curve, as that cycle in which the fluorescence reaches 10 SD above the mean of the general background (Fig. 1b). A Ct of 40 means that there was no fluorescence detected in that sample after 40 cycles of PCR, therefore the gene of interest was not present in the sample or was too low to be detected. The formula for the standard curves is Ct $= m \times (\log_{10}$ copies$) + b$, where the slope (m) reflects the efficiency of replication for a particular pair of primers and the Y-intercept (b) reflects the sensitivity of detection for a particular probe. When we plotted the Ct for each sample of our gene standards against the $\log_{10}$ of the copy number, the curves had a slope between $-3.18$ and $-3.32$ (Fig. 1c) approaching the maximal theoretical efficiency of the PCR (perfect doubling at each cycle = $-3.33$). This indicated that our chosen primers were nearly maximally efficient. Further, the extrapolated Y-intercepts lay near 40 cycles, indicating that the lower level of detection for each combination of primers and probes was between one and one hundred copies of the relevant gene.

To test the ability of this technique to measure $\beta$-gal-specific immune reactivity in the absence of any expansion or in vitro culture steps, we injected two mice i.v. with 10$^7$ PFU of $\beta$FPV and two mice with the same amount of non-$\beta$-gal-carrying cFPV, boosted them 14 days later with 10$^7$ $\beta$VV or cVV, respectively,
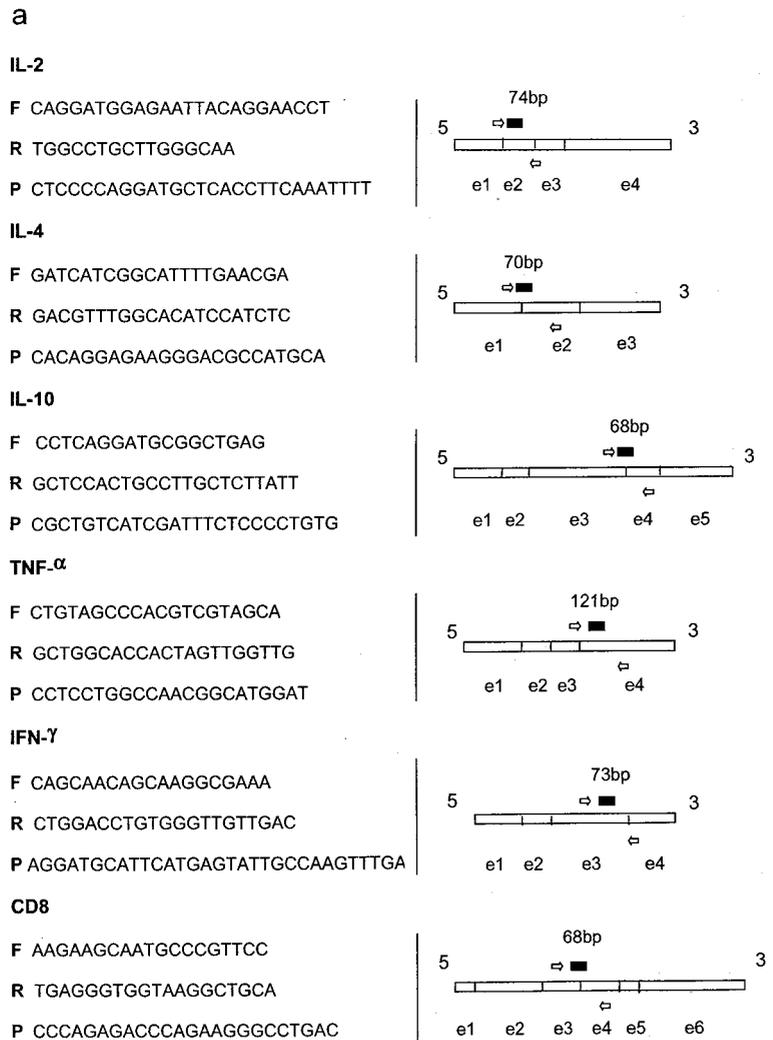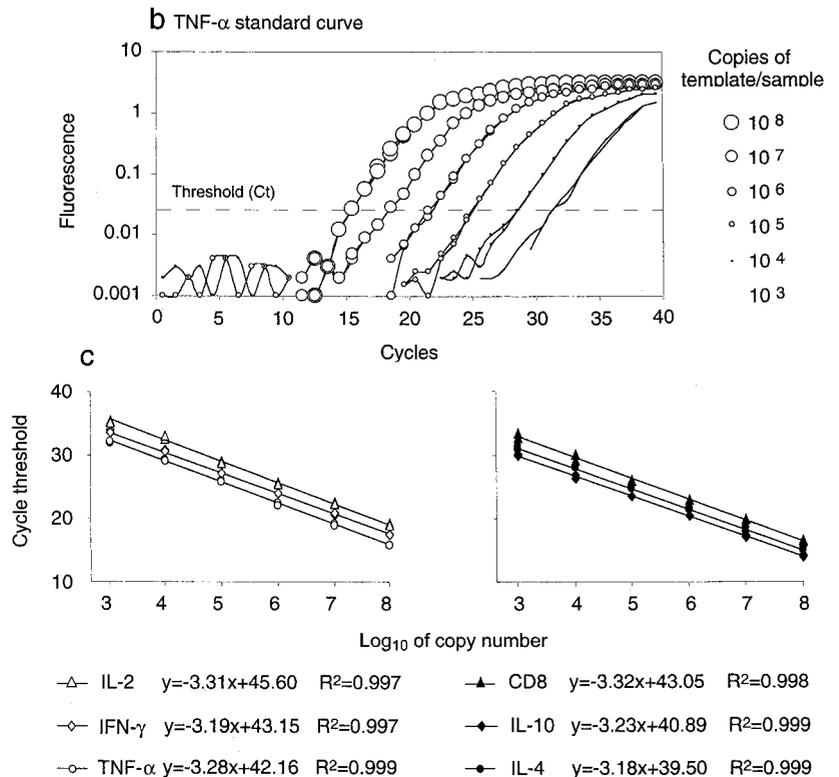
**FIGURE 1.** Primers and probes designed for quantitative RT-PCR of murine *IL-2*, *IL-4*, *IL-10*, *TNF-α*, *IFN-γ*, and *CD8* genes. *a*, F, forward primers, and R, reverse primers were used at 200 nM; P, probe was used at 100 nM and was labeled at the 5′ end with the reporter dye molecule 6-carboxyfluorescein and at the 3′ end with the quencher dye molecule 6-carboxytetramethylrhodamine. The figure shows the position of the primers and probes with respect to the exon (e)-intron junctions and the base pair number of each amplicon. *b*, Amplification plot obtained after quantitative PCR of 10-fold dilutions of *TNF-α* amplicon used to generate its standard curve. Dilutions (from $10^8$ to $10^3$ copies of templates per sample) were amplified in duplicate and are represented as gradually diminishing open circles, the largest corresponding to $10^8$ and the line without circles to $10^3$ copies per sample. *c*, Standard curves from quantitative PCR of serial dilutions of standard template copies of each gene. Overlapping points on standard curves represent templates assayed in duplicate. The equations represent the regression lines for each gene.



a

**IL-2**

F CAGGATGGAGAATTACAGGAACCT

R TGGCCTGCTTGGGCAA

P CTCCCCAGGATGCTCACCTTCAAATTTT

74bp

e1 e2 e3 e4

**IL-4**

F GATCATCGGCATTTTGAACGA

R GACGTTTGGCACATCCATCTC

P CACAGGAGAAGGGACGCCATGCA

70bp

e1 e2 e3

**IL-10**

F CCTCAGGATGCGGCTGAG

R GCTCCACTGCCTTGCTCTTATT

P CGCTGTCATCGATTTCTCCCCTGTG

68bp

e1 e2 e3 e4 e5

**TNF-α**

F CTGTAGCCCACGTCGTAGCA

R GCTGGCACCACTAGTTGGTTG

P CCTCCTGGCCAACGGCATGGAT

121bp

e1 e2 e3 e4

**IFN-γ**

F CAGCAACAGCAAGGCGAAA

R CTGGACCTGTGGGTTGTTGAC

P AGGATGCATTCATGAGTATTGCCAAGTTTGA

73bp

e1 e2 e3 e4

**CD8**

F AAGAAGCAATGCCCGTTCC

R TGAGGGTGGTAAGGCTGCA

P CCCAGAGACCCAGAAGGGCCTGAC

68bp

e1 e2 e3 e4 e5 e6

b TNF-α standard curve

Copies of template/sample

○ $10^8$

○ $10^7$

○ $10^6$

○ $10^5$

· $10^4$

$10^3$

c

Log10 of copy number

—△— IL-2 y=-3.31x+45.60 R²=0.997

—◇— IFN-γ y=-3.19x+43.15 R²=0.997

—○— TNF-α y=-3.28x+42.16 R²=0.999

—▲— CD8 y=-3.32x+43.05 R²=0.998

—◆— IL-10 y=-3.23x+40.89 R²=0.999

—●— IL-4 y=-3.18x+39.50 R²=0.999

and harvested the splenocytes 7 days later. We rested $5 \times 10^5$ splenocytes/well overnight in 96-well plates in the absence of growth factors and stimulated the splenocytes the following day for 2 h with the H-2L$^d$-restricted β-gal peptide or the β-gal-expressing tumor F6 cells. As controls, the splenocytes were stimulated with a peptide from influenza (Flu) that is also presented by H-2L$^d$ Ags or with the β-gal-negative parental tumor cells, CT26. We calculated β-gal-specific reactivity as the ratio of IFN-γ mRNA to CD8 mRNA in β-gal-stimulated wells vs control (Flu or CT26)-stimulated wells.

Table I shows the cytokine production pattern in splenocytes from one representative mouse of two tested, after 2 h of in vitro sensitization with β-gal or Flu peptide. No β-gal-specific *IL-2*, *TNF-α*, or *IFN-γ* mRNA production could be detected in mice vaccinated with control viruses (ratios β-gal/Flu were <2). However, a significant amount of β-gal-specific *IFN-γ* transcript was detected in splenocytes of β-gal-vaccinated mice. For example, the number of copies of mRNA found in the β-gal stimulated sample of a vaccinated mouse (247,035), when normalized to the copies of mRNA detected for *CD8* in the same well (25,442), equals 9.7. This number represents the IFN-γ production, with respect to the number of CD8 cells, upon stimulation with the β-gal CD8 epitope. When compared with the IFN-γ production in splenocytes from the same mouse stimulated with the control Flu CD8 epitope (5,705 copies of IFN-γ:20,339 copies of CD8 = 0.28), it is clear this vaccinated mouse makes a 35-fold stronger response to β-gal than to Flu. The ratio of β-gal-Flu calculated for the second β-gal vaccinated mouse was 51. Production of IL-2 and TNF-α in the β-gal and Flu stimulated samples were calculated in the same way using their own standard curves (Fig. 1c) to extrapolate the cytokine gene copy number from the Ct. As previously seen in PBMCs from vaccinated patients (12), IL-2 and TNF-α mRNA were also specifically produced by splenocytes of β-gal vaccinated mice, although to a lower degree than IFN-γ (ratios of 4.8 and 4.0 β-gal specific-Flu specific, respectively, for the first mouse, and ratios of 25 and 3.3, respectively, for the second mouse). As expected for responses to FPV, no specific IL-10 or IL-4 production was detectable.

Because none of the presently used ex vivo methods to detect the immune response tests the susceptibility of tumor cells to immune recognition and destruction, we designed primers and probes for perforin and granzyme A to assess specific cytotoxic function in vaccinated mice. These proteins are known to be involved in the lytic function of CTL. In freshly isolated splenocytes, mRNA for these genes was elevated in vaccinated mice. However, there was no change in level in response to β-gal sensitization in an 8-h in vitro kinetic study (data not shown), suggesting that in activated CTL, the release of these effectors molecules is most likely modulated at the posttranscriptional level. Because of its response to vaccination and to short-term in vitro stimulation, we selected IFN-γ as the most sensitive marker for the detection of β-gal-specific responses ex vivo.

*The vaccine system: anti-β-gal reactivity rises in response to gradual increases in vaccine dose and number*

We next evaluated a spectrum of vaccine doses to determine whether there is a range in which the response would vary proportionally with the dose. We vaccinated seven groups of mice i.v. with different amounts of βFPV (three mice per group received $10^2$ or $10^3$ PFUs and five mice per group received from $10^4$–$10^8$ PFUs). Seven days later, we tested the splenocytes from one mouse per group to quantify specific β-gal reactivity by qRT-PCR-based measurement of IFN-γ expression after stimulation with β-gal peptide or the F6 tumor, as described above. To determine whether a second dose would influence the response, we boosted two mice from each experimental group i.v. 14 days after the first vaccination. As it is thought that the Ab response to a viral vector may inhibit its efficacy (20), we changed to a vaccinia recombinant, each boosted mouse receiving a dose of βVV equivalent to the dose of βFPV with which it had been previously vaccinated (from $10^2$ to $10^8$ PFUs). As controls, two mice from each experimental group that had received $10^4$ to $10^8$ PFUs of βFPV were injected with corresponding PFUs of control cVV instead of βVV. Seven days after the last vaccination, we measured the specific β-gal response from the splenocytes of these mice.

We found that, after a single vaccination, the magnitude of the immune response began to increase with incrementally increasing viral doses above $10^5$ PFUs and had not yet reached a plateau at doses of $10^8$ PFUs (Fig. 2a); this did not improve, and may have been somewhat inhibited by, boosting with a control vaccinia vector (Fig. 2b). In response to a second vaccination with βVV, groups given $10^5$ or more PFUs reached plateau levels of IFN-γ

**Table I.** *Ex vivo quantification of cytokine mRNA production in control and β-gal-vaccinated mice after peptide sensitization of splenocytes*

| Vaccine[a] | β-gal[b] | | | Flu[b] | | | Ratio β-gal/Flu[f] |
|---|---|---|---|---|---|---|---|
| | Ct[c] | Copies cDNA[d] | Copies cytokine/CD8[e] | Ct[c] | Copies cDNA[d] | Copies cytokine/CD8[e] | |
| β-gal vector | | | | | | | |
| IL-2 | 33.7 | 1,229 | 0.048 | 35.6 | 204 | 0.01 | **4.8** |
| TNF-α | 32.1 | 207 | 0.008 | 33.9 | 42 | 0.002 | **4.0** |
| IFN-γ | 27.8 | 247,035 | 9.709 | 33.7 | 5,705 | 0.281 | **34.6** |
| IL-4 | 40 | 0 | | 40 | 0 | | |
| IL-10 | 37 | 175 | 0.007 | 38.1 | 83 | 0.004 | 1.8 |
| CD8 | 30.8 | 25,442 | | 31.1 | 20,339 | | |
| Control vector | | | | | | | |
| IL-2 | 34.6 | 529 | 0.009 | 34.7 | 458 | 0.014 | 0.6 |
| TNF-γ | 33.3 | 74 | 0.001 | 33.4 | 64 | 0.002 | 0.5 |
| IFN-γ | 34.1 | 2,909 | 0.048 | 34.4 | 3,665 | 0.11 | 0.4 |
| CD8 | 29.4 | 60,915 | | 30.4 | 33,390 | | |

[a] Mice were vaccinated twice with control virus or β-gal-carrying virus and sacrificed 7 days after the second vaccination.
[b] Splenocytes were stimulated for 2 h with 1 μM of flu or β-gal peptide after which the RNA from the different wells was extracted and qRT-PCR was performed.
[c] Ct, average of duplicates.
[d] Number of cDNA copies obtained from extrapolation of the Ct number to the standard curve for each gene.
[e] Copy number of the cytokine divided by the copy number of the reference gene (*CD8*) in each sample.
[f] Represents how many times the cytokine gene was expressed in the β-gal vs control (Flu)-stimulated samples after normalization for *CD8* expression.
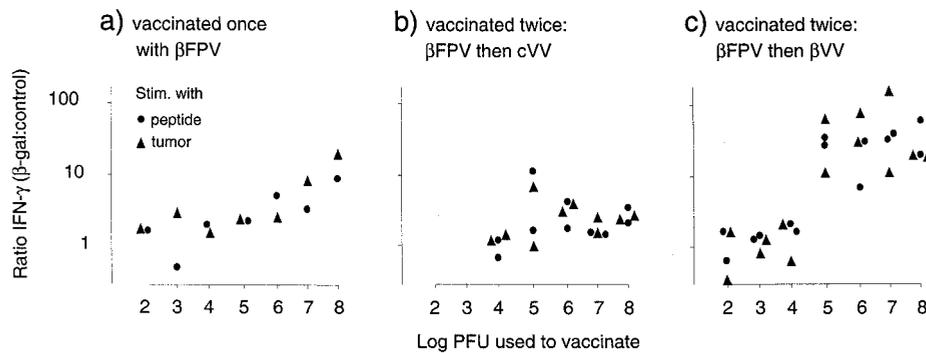
**FIGURE 2.** Ex vivo detection of $\beta$-gal reactivity after one or two vaccinations with a gradually increased dose of $\beta$-gal-carrying vectors. Thirty-one mice were divided into seven groups receiving i.v. different amounts of $\beta$FPV (three mice per group receiving $10^2$ or $10^3$ PFUs and five mice per group receiving from $10^4$ to $10^8$ PFUs). Seven days later, one mouse per group was sacrificed to ex vivo quantify $\beta$-gal reactivity in the spleen. Fourteen days after the first vaccination, two mice from each experimental group were boosted i.v. with $\beta$VV by administering the same PFUs that they had received when vaccinated previously with $\beta$FPV (from $10^2$ to $10^8$). The rest of the mice (from groups vaccinated previously from $10^4$ to $10^8$ PFUs of $\beta$FPV) were injected with corresponding PFUs of cVV. Seven days after the last vaccination, mice were sacrificed to ex vivo quantify $\beta$-gal reactivity in the spleen. $\beta$-gal reactivity was quantified by stimulating $5 \times 10^5$ splenocytes with $\beta$-gal epitope (1 $\mu$M) or with the $\beta$-gal-positive clone C25.F6 ($10^5$ cells). As controls, splenocytes were incubated with the same concentration or number of Flu epitope or the $\beta$-gal negative cell line CT26, respectively. After 2 h of sensitization, RNA was extracted from every well and qRT-PCR was conducted to determine whether IFN-$\gamma$ mRNA production normalized to CD8 mRNA for each well. Stimulation was conducted for 2 h either with peptide or tumor cells, based on previous kinetic studies suggesting that the peak of IFN-$\gamma$ transcript expression occurs within 2–3 h (data not shown). Ratio IFN-$\gamma$ was calculated as described in Table I. *a,* The ratio of IFN-$\gamma$ from one mouse per group after $\beta$FPV vaccination. *b,* The ratio of IFN-$\gamma$ from two mice per group after a second vaccination with cVV. *c,* The ratio of IFN-$\gamma$ from two mice per group after a second vaccination with $\beta$VV. Circles and triangles represent the ratio of IFN-$\gamma$ after peptide and tumor sensitization, respectively.

production that were 5–20 times higher than mice given a single vaccination (Student's *t* test, $p = 0.05$ for PFU $\geq 5$; Fig. 2*c*). Thus, using direct ex vivo measurements, we found that doses between $10^3$ and $10^7$ PFUs of $\beta$-gal-carrying vectors represented a frequency and range of vaccination that resulted in significant differences in vaccine-specific immune responsiveness, as measured directly ex vivo.

*Tumor regression correlates with ex vivo detection of vaccine-elicited immune responsiveness*

To test whether the incremental changes in vaccine-induced responsiveness, as measured by IFN-$\gamma$ production ex vivo, have any meaningful correlation with in vivo anti-tumor activity, we tested our vaccine protocols on mice carrying a tumor that expresses $\beta$-gal. Previous studies with the $\beta$-gal-expressing tumor CT26.CL25 have shown that vaccination with $\beta$-gal-expressing viral vectors can have some effect on tumor growth. However, the effects were not complete, as 20% of the tumors eventually grew out, despite vaccination (20). After analyzing these studies, we considered the possibility that the $\beta$-gal-transfected cell line that had been used might not have comprised a clone of stably transfected cells but a mixed population from which nontransfected cells, or perhaps loss variants, might have escaped from the vaccine-induced immune response. This might have obscured the relationship between vaccination and tumor rejection. In fact, when we looked at $\beta$-gal expression in cell line CT26.CL25 cultured in the presence (Fig. 3*a*) or absence (Fig. 3*b*) of selection medium, we detected a cell population that completely lost $\beta$-gal expression when line CT26.CL25 was cultured without G418 (Fig. 3*b*). Therefore, we set out to determine whether we could select for a stable $\beta$-gal expressing clone of CT26.CL25 with which to continue our vaccination study. We first selected, by FACS sorting and single cell cloning, several cells among the top 1% of the highest $\beta$-gal expressors. We grew the resulting clones without G418 selection medium to allow unstable clones to lose expression, then we sorted again. Fig. 3, *c* and *d,* demonstrates the levels of $\beta$-gal expression by clone CT26.CT25.F6 7 days and 2 mo after the second sorting when cultured in the absence of selection me-

dium. Although the level of $\beta$-gal expression dropped somewhat-,the cells did not completely lose $\beta$-gal expression, even after prolonged in vitro culture without selective agents, suggesting a decreased likelihood that it would lose $\beta$-gal expression during a similar period of in vivo growth. Therefore, we chose clone F6 to continue our vaccination study.

To test whether the vaccine-induced immune response, as measured by ex vivo IFN-$\gamma$ production, correlates with tumor rejection, we injected incrementally increasing primary and boosting doses of $\beta$-gal vectors, as in Fig. 2*c*, into mice bearing 3-day-old pulmonary metastases of clone F6. Seven days after the last vaccination, we sacrificed the mice, counted the number of pulmonary metastases, and measured the IFN-$\gamma$ response against $\beta$-gal from their splenocytes. Results from two similar experiments (Fig. 4) show that there was a clear dose response in effective tumor clearance, as the number of metastases dropped with escalating doses of $\beta$-gal-carrying vaccine vectors. Moreover, this correlated with a concomitant increase in specific IFN-$\gamma$ production against $\beta$-gal peptide and the F6 tumor that was measured in randomly selected mice from each treatment group. Notably, there was a significant amount of variability in specific IFN-$\gamma$ production among mice in the same treatment group and this variability revealed that the strength of the measured ex vivo response correlated more closely with in vivo tumor immunity than we might have expected from a simple dose escalation trial. For example, in experiment one, one mouse in the group vaccinated with $10^2$ PFUs (designated by $\triangle$) made no specific IFN-$\gamma$ in response to $\beta$-gal (Fig. 4*b*; a ratio of 1.1) and had 35 metastases whereas another in the same group ($\bigcirc$) had a specific IFN-$\gamma$ ratio of 2.8 and no metastases. Such correlations suggest that different individuals respond differently to a particular dose of vaccine and that ex vivo IFN-$\gamma$ production is a good representation of the in vivo response to the tumor.

Because the route of administration can affect the immune response to a vaccine, we also tested the i.p. route. Again the responses titrated with escalating doses of vaccine (Fig. 5), although i.p. injection was ~10-fold less efficient than i.v. administration. As measured by direct ex vivo IFN-$\gamma$ mRNA expression, the response to $\beta$-gal was first detected in mice vaccinated with $10^4$
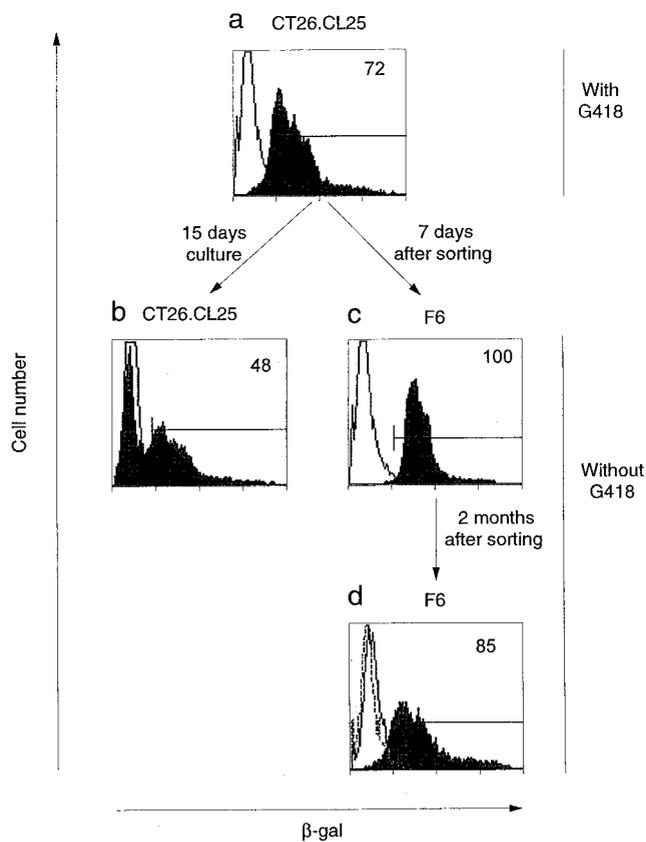
**FIGURE 3.** Stable β-gal expression by the F6 clone compared with the CT26.CL25 cell line. The CT26.CL25 cell line, derived from the CT26 cell line after transfection with the *β-gal* gene, and the F6 clone, derived from the CT26.CL25 cell line after two consecutive rounds of sorting, were analyzed by FACS for β-gal expression using FDG staining after being in culture in the presence (CT26.CL25) or absence (both) of selection medium. *a,* β-gal expression of CT26.CL25 cell line cultured in presence of G418. *b,* β-gal expression of the same line after 15 days of in vitro culture without G418. *c,* β-gal expression of clone F6 7 days after the second round of FACS sorting of high β-gal-positive cells from *a. d,* β-gal expression of the same clone after 2 mo of in vitro culture without selection medium. The empty continuous line represents the FDG-stained CT26 cell line. The discontinuous line represents unstained F6 clone. Numbers in the *upper right corner* of the histograms represent the percentage of β-gal-positive cells.

PFUs. By this route of vaccination, the ex vivo test again correlated very well with tumor rejection, as those groups responding more strongly also contained fewer tumor metastases.

Finally, we pooled data from different experiments to study the relationship between tumor disappearance and the two variables under study in these experiments: vaccine dose and the ex vivo detection of specific IFN-γ mRNA production. To better compare the antitumoral effect among mice from different experiments, we normalized the number of metastases carried by each mouse to the average of metastases in the untreated control group from the same experiment. Fig. 6a shows the relationship between tumor treatment and vaccine dose in mice vaccinated twice i.v. (●) or i.p. (○) with β-gal-carrying vectors, while Fig. 6b shows the relationship between tumor treatment and ex vivo-specific IFN-γ production. This plot includes mice vaccinated with different doses and numbers of β-gal vaccines and using different routes of administration (i.p., ○; i.v., ●). Overall, it is clear that there is a strong correlation between the dose of administered vaccine, the ex vivo IFN-γ response, and the reduction in tumor metastases, whether the vaccine

was given i.v. or i.p. There are two noteworthy features apparent in this summary. The first is that (perhaps not surprisingly), the route of vaccination had a strong impact, both on ex vivo responsiveness, and on reduction of tumor load. i.v. administration was 10 to 100-fold more effective than i.p. The second is that individual animals reacted quite differently to the same dose of vaccine, even though they were age-matched members of the same inbred strain. This variation underscored the value of measuring the ex vivo production of IFN-γ, as it showed that IFN-γ production correlates more closely with tumor reduction than does vaccine dose, number, or route of administration. For example, the mouse inside an open diamond made an Ag-specific ratio of 2.8 IFN-γ units and completely rejected the tumor, although it had only received the lowest dose of $10^2$ PFU of β-gal-viruses. In contrast, the mice inside open triangles showed poor anti-tumor effect (lung metastases = 81 and 80% of controls), although one received $10^2$ PFU of β-gal viruses (small triangle) and the other one received 10 times more (large triangle). However, their specific IFN-γ responses were similarly low (ratio IFN-γ = 0.5 and 0.9, respectively). The correlation is equally striking in mice vaccinated by the i.p. route. Although this form of vaccination was 10 to 100-fold less effective than i.v. administration, the correlation with IFN-γ production was indistinguishable from that of mice that had been vaccinated i.v. For example, though the two mice delineated by circles were given $10^3$ PFU i.v. (small circle) or $10^5$ PFU i.p. (large circle), they made similar ratios of 2.8 and 3.1 IFN-γ units and rejected their tumors. In the middle ranges, though the two mice delineated by squares were given $10^2$ PFU i.v. (small square) or $10^4$ PFU i.p. (big square), they showed weak ex vivo specific IFN-γ production of 1.4 and 1.7 units, respectively, and weak anti-tumor effectiveness with 65 and 30% of lung metastases, respectively. These data show that the immediate ex vivo measurement of Ag-specific IFN-γ production is an excellent representation of the effective in vivo anti-tumor response.

## Discussion

Clinicians have long sought an in vitro assay that accurately represents the in vivo immune response of vaccinated patients. In previous studies, we had found that the immediate ex vivo measurement of tumor-specific production of IFN-γ did not seem to correlate with the progression of tumors in vaccinated patients. In many cases, the tumors persisted despite measurable vaccine-induced immunity while in others, the tumors remained static or regressed in the absence of a large IFN-γ response (12). Although the possibility existed that there truly was no connection between our in vitro measurement and the in vivo response, we hypothesized that other confounding features (such as patient variability, tumor heterogeneity, and the immunosuppressive effects of prior anti-tumor therapies) might be obscuring the picture. To determine, in principle, whether the strength of the in vivo response to a tumor vaccine can be measured by an immediate ex vivo assay, whether this measurement has any relevance to tumor clearance and whether the response can be manipulated by varying the parameters of vaccination, we created a simple mouse model in which several technical details allowed us to minimize the kind of variability that is seen with human patients. First, we used age-matched inbred (BALB/c) mice to minimize host variability. Second, we used a cloned and recloned β-gal-transfected tumor to minimize tumor heterogeneity. Transfected cell lines are initially notoriously unstable and, in some previous studies, the transfected tumors may have been mixed populations at the time of injection
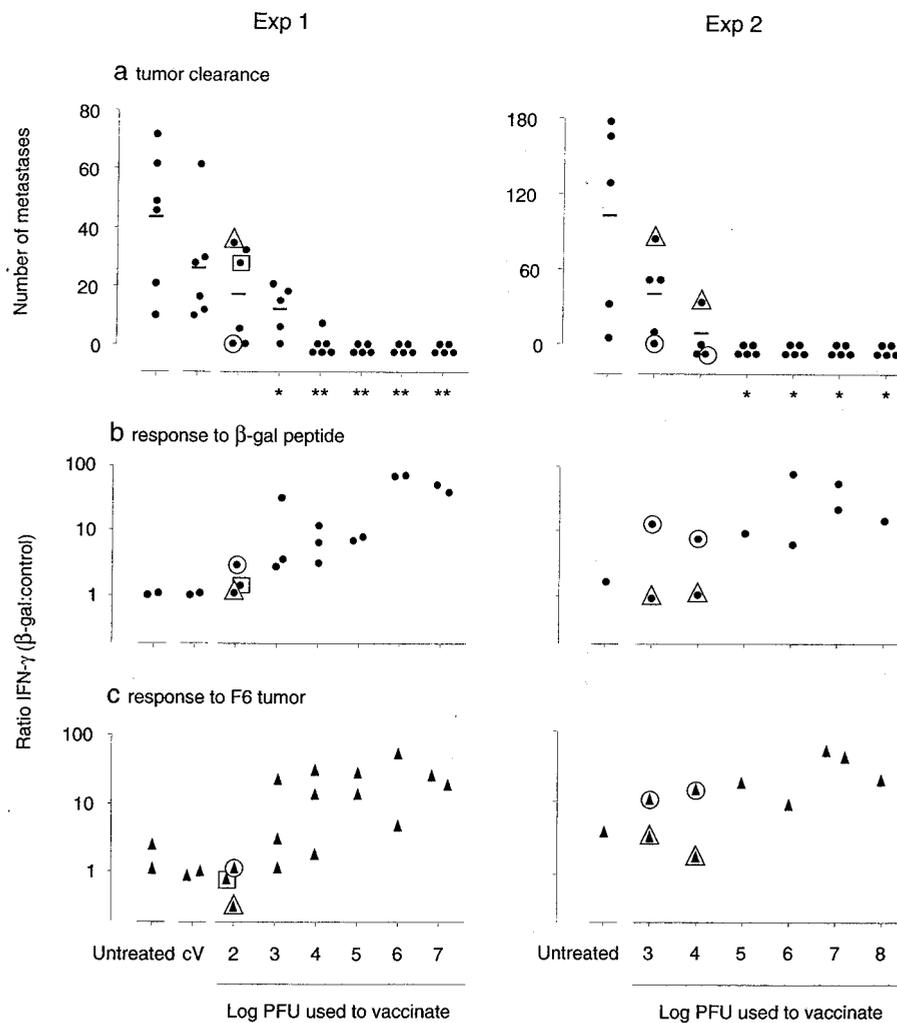
**FIGURE 4.** Mice with higher β-gal-specific immune responses reject β-gal-expressing tumors. Two experiments were performed in a similar way with slight variations in the number of mice per group and treatment groups. Forty-four and 34 mice (experiment one and two, respectively) were challenged i.v. with $10^5$ F6 tumor cells. Three days later, the mice in experiment one were divided into eight treatment groups: untreated ($n = 6$); vaccinated with $10^7$ PFUs of control virus, cFPV ($n = 6$); vaccinated i.v. with increasing doses of βFPV ($n = 6$ for doses of $10^2$ and $10^4$ PFUs and $n = 5$ for doses of $10^3$, $10^5$, $10^6$, and $10^7$ PFUs). The mice in experiment two were divided into seven treatment groups: untreated ($n = 5$); vaccinated i.v. with increasing doses of βFPV ($n = 5$ for doses of $10^3$, $10^5$, $10^6$, $10^7$, and $10^8$ and $n = 4$ for $10^4$). Twelve days after the primary vaccination, the vaccinated mice were boosted with the same dose of βVV (for βFPV primed mice), or of cVV for the control group. Seven days later, the mice were sacrificed, their lungs were coded, and metastases were enumerated by an observer ignorant of the code. Spleens from between one and three mice per treatment group were removed and analyzed for ex vivo specific IFN-γ mRNA production as described in the *Materials and Methods* section. *a,* The number of lung metastases per mouse in each treatment group. The horizontal line represents the average of lung metastases. * or **, Treatment group with significantly ($p < 0.05$) or very significantly ($p < 0.01$) fewer metastases than the untreated group. *b,* The ratio of IFN-γ between β-gal and Flu peptide-sensitized cells. *c,* The ratio of IFN-γ between F6 and CT26 tumor-sensitized cells. The ratio of IFN-γ was calculated as described in Table I. In each experiment, the same kind of open symbol (triangle, square, or circle) per treatment group represents the same mouse, where both lung metastases and ex vivo anti-β-gal activity (against CD8 epitope and F6 clone) in the spleen were quantified.

(20, 24–26). Thus, tumor outgrowth might as easily have been due to escape by cells that had never expressed the transfected gene as to mutants that had lost expression. By selecting a stable transfectant and recloning it several times, we minimized the outgrowth of non-Ag-expressing tumors. Third, to minimize the potentially suppressive effect of Ab to the viral vectors, we used different viral vectors for the primary and secondary vaccinations. Fourth, we took advantage of the sensitivity of real-time qRT-PCR to measure the ex vivo response of vaccinated cells after only 2 h of stimulation in vitro. We used spleens as the source of T cells because they are the closest mouse source to human PBL (the ones generally tested in vaccinated patients) that gave us the required number of cells for this assay. Unlike standard in vitro assays, this short period is insufficient to allow naive T cells to become producers of

IFN-γ or to allow cell division and is thus likely to be a fairly accurate measure of the number and/or frequency of currently active vaccine-induced tumor-specific cells.

With this system, we found that 1) effective in vivo antitumor immunity can indeed be manipulated by changing the dose, incidence, or route of vaccination; 2) regardless of the route, frequency, or dose, and despite great variability in the responses of individual animals to any particular vaccination protocol, the ex vivo production of IFN-γ, as measured by qRT-PCR after a 2-h Ag pulse, correlated very well with the in vivo anti-tumor response; and 3) low responses, though easily detectable ex vivo, were often not sufficient to clear the tumor.

The single most important feature of this study was the finding that the simple presence of a measurable immune response was not
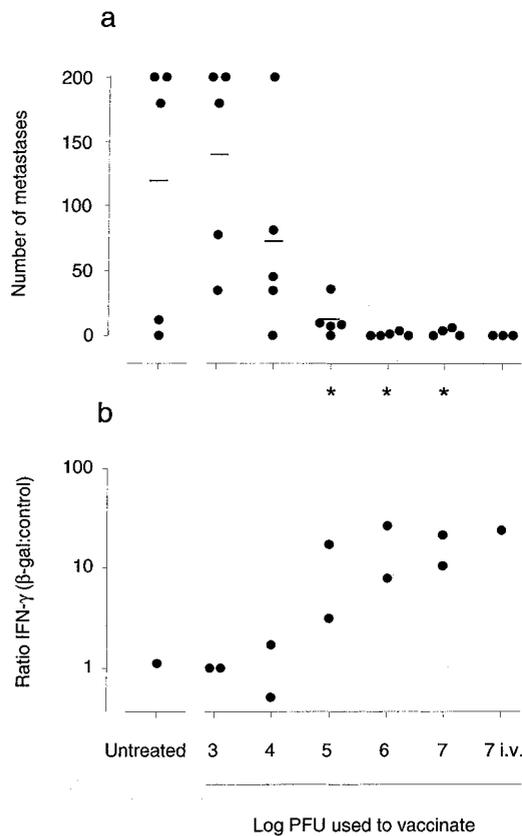
a



b



Log PFU used to vaccinate

**FIGURE 5.** Mice with higher specific immune responses generated by i.p. vaccination reject $\beta$-gal-expressing tumors. Thirty-two mice were challenged i.v. with $2 \times 10^5$ F6 tumor cells. Three days later, mice were divided into six treatment groups: untreated ($n = 6$), and vaccinated i.p. with increasing doses of $\beta$-gal viruses ($n = 5$ for doses of $10^3$, $10^4$, $10^5$, and $10^6$ cells; $n = 4$ for $10^7$ PFUs). One small group ($n = 3$) received two i.v. vaccinations with $10^7$ PFUs of $\beta$-gal viruses as a positive control. The rest of the experiment was performed in the same manner as described in Fig. 4. *a,* The number of lung metastases per mouse in each treatment group. The horizontal line represents the average of lung metastases. *, The treatment group with significantly less numbers of metastases ($p < 0.05$) than the untreated group. *b,* The ratio of IFN-$\gamma$ between $\beta$-gal and Flu peptide-sensitized splenocytes from two mice from each group, except from untreated and i.v.-treated groups, where one mouse was tested. The ratio of IFN-$\gamma$ was calculated as described in Table I.

a



Log PFU used for vaccination

b

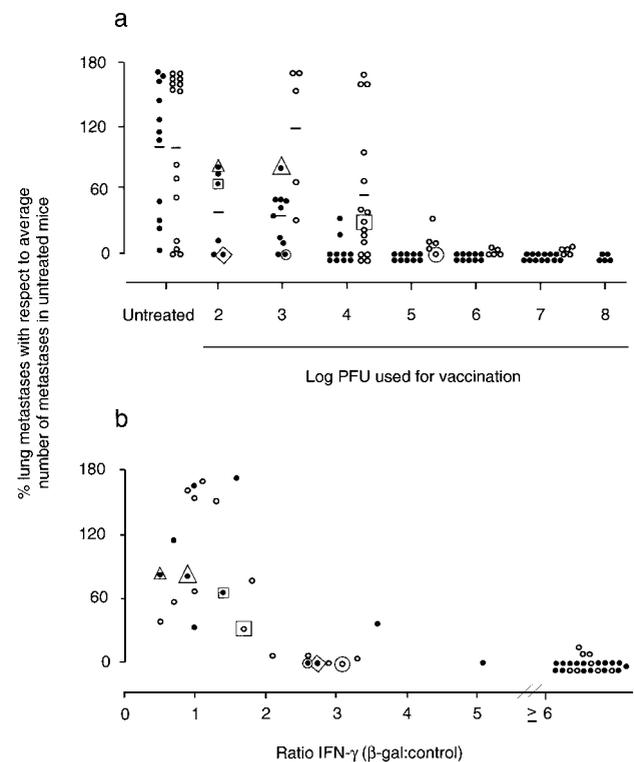

Ratio IFN-$\gamma$ ($\beta$-gal:control)

**FIGURE 6.** Ex vivo tumor Ag-specific CD8 activity better correlates than the vaccine dose with tumor rejection. *a,* The number of metastases with respect to the vaccine dose in mice vaccinated with $\beta$-gal-carrying vectors i.v. ($n = 75$, filled circle) or i.p. ($n = 50$, open circle) in data pooled from three individual experiments (Figs. 4 and 5). Horizontal lines represent the average of lung metastases in vaccinated mice. *b,* Number of metastases with respect to ex vivo-specific IFN-$\gamma$ mRNA production in 49 mice from 4 individual experiments where the route and dose of vaccination varied. The ratio of IFN-$\gamma$ refers to ex vivo $\beta$-gal peptide sensitization and was calculated as described in Table I. The percentage of lung metastases with respect to the average metastases in untreated mice is the number obtained after dividing the number of metastases found in each mouse by the average number of metastases in untreated mice from the same experiment and multiplying by 100. The same delineating symbol in *a* and *b* represents the same mouse.

always sufficient to clear a tumor, but that the strength of the response was critical. Tumor outgrowth in the presence of immunity is not a new finding. For example, tumor-infiltrating lymphocytes can be isolated from growing tumors and shown to have anti-tumor specificity; tumor-specific immunity can be shown in vaccinated patients, though their tumors continue to grow and many vaccine strategies have failed to clear tumors, though immunity was clearly established. These failures of immunity have been variously attributed to outgrowth by tumor Ag or MHC Ag loss variants (27), to tumor expression of immune response inhibitory cytokines like TGF-$\beta$ (28) or apoptotic signals like Fas ligand (29), and to the establishment of a resistant tumor microenvironment (30). However, in our study, the instability in tumor Ag expression by the tumor was minimized and none of the other factors seemed to be major problems. Although we allowed the tumor to establish itself before vaccinating, we did not find that it was able to establish a protected microenvironment in 3 days. Instead, we saw that, if the immune response was strong enough, as measured by ex vivo production of IFN-$\gamma$ the tumors were almost invariably cleared.

The relationship between strength of response and its efficacy at rejecting a tissue has been known for some time in transplant situations, where grafts that differ by a "weak" minor histocompatibility Ag can take a very long time to reject and are often accepted by a proportion of recipients, even though these recipients clearly become immunized and are able to rapidly reject subsequent grafts (31, 32). In these cases, small grafts are rejected more often than large ones. In the case of a rapidly growing tumor, a weak immune response, though measurable ex vivo, would simply not be able to catch up.

Thus, it is clear that any vaccine programs designed to treat tumors should not rely simply on measurements of the presence or absence of vaccine-elicited immunity. They must take into account the strength of the elicited immune response in vivo and design the vaccination route and schedule to bring the response up to an effective level. This requires assays that accurately measure the strength of an ongoing response, but the majority of assays in current use do not do that. There are three major classes of such assays: 1) those that measure the number of cells that can bind to a particular Ag (such as MHC/Ag tetramer binding assays). These assays, while useful in determining the number of Ag-specific cells, may or may not reflect the functional status of those cells,

nor do they measure the number of cells able to recognize other Ags on a tumor; 2) assays that measure the precursor frequency of Ag-specific memory cells for a particular function (such as limiting dilution CTL assays). These types of assays, with their long culture periods, are a measure of clonable memory cells that do not give a clear picture of the currently ongoing activity state of the responding cells in vivo; and 3) assays that attempt to measure the level of currently active lymphocytes immediately ex vivo (such as short-term intracellular cytokine assays, short-term ELISPOT assays, and short-term qRT-PCR). These latter assays have the potential to represent, reasonably accurately, the ongoing in vivo response and therefore can give the type of information needed to determine whether the elicited response is strong enough or needs to be enhanced. Although in this study we did not compare the real-time PCR-based assessment of immune response with other methods, we have previously noted a good correlation with results obtained in clinical settings using tetrameric HLA/epitope complexes and intracellular cytokine staining (15).

Although the production of IFN-$\gamma$ correlated well with tumor clearance in this study and an IFN-$\gamma$-dependent mechanism has also been shown to be effective against the B16 melanoma cells (33), there are several reasons why assays of other cytokines may be best in other situations. First, some tissues are exquisitely sensitive to Th1 cytokines such as TNF-$\alpha$ and IFN-$\gamma$ like pancreatic islets (34), placenta (35), and eye (36), whereas others are more resistant. Thus, a vaccine-elicited IFN-$\gamma$ response may be entirely appropriate to clear some tumors, but useless against others. Second, though IFN-$\gamma$ and CTL often occur concomitantly, there is evidence that the two can also occur independently (37). For tumors where a CTL response is necessary, measurement of IFN-$\gamma$ may give an accurate assessment in some patients and not in others. In these cases, direct measurement of the killing function, or of granzyme or perforin, might be more appropriate. In the present study, we found that the levels of these molecules were indeed higher in vaccinated than in control animals. However, they did not increase in a 2-h stimulus with Ag or with tumor, suggesting that effector cells control their release by other, posttranscriptional, means. Thus, it may be necessary to find the best correlate for each vaccine protocol and each type of tumor. In each case, it will be important to insure that the assay measures the strength of the ongoing in vivo response rather than its mere presence.

Our study shows that, in principle in mice, the strength of a vaccine-elicited response is critical to its efficacy in clearing a tumor, that it can be manipulated by varying the dose, frequency and route of vaccination, and that it can be accurately measured by an immediate ex vivo method. In light of these data, we re-examined our earlier study on vaccinated human patients. Though the overall correlation between tumor regression and ex vivo response was low, we did find that there was tumor regression and/or stasis in the small number of patients who made very strong IFN-$\gamma$ responses. In addition, data from various immunization methods tested at our institution suggest that the vaccination schedule associated with the highest success rate in inducing ex vivo immune responses is also the most effective clinically (Ref. 38 and unpublished data). Thus, although at the individual patient level it might be difficult to directly relate the intensity of immune response to clinical outcome, larger population-based studies may yield information comparable to the mouse model. Inaccuracy in the correlation between in vitro immunity and clinical effects in human studies may reflect different suitability of tumor cells as targets for effector T cells as tumors are quite heterogenous in HLA and/or tumor Ag expression (27). Finally, the timing in which immune responses have been documented in human studies has been quite

arbitrary, as knowledge of the kinetics of vaccine-induced cellular responses in humans has not been comprehensively studied.

Recently, we followed the kinetics of TCR use in response to repeated epitope-specific vaccination in a limited cohort of patients. This preliminary study suggested that increasing the number of vaccinations broadens and intensifies the extent of the immune response (39). Based on this human study and the findings described in this mouse model, we have begun a trial in which patients with advanced cancer are repeatedly boosted to test whether 1) higher precursor frequency of cancer-specific T cells can be generated and 2) improved clinical outcome will follow this enhancement of the immune response.

## Acknowledgments

## References
1. Boon, T., P. G. Coulie, and B. Van den Eynde. 1997. Tumor antigens recognized by T cells. *Immunol. Today 18:267.*
2. Rosenberg, S. A. 1997. Cancer vaccines based on the identification of genes encoding cancer regression antigens. *Immunol. Today 18:175.*
3. Old, L. J., and Y. T. Chen. 1998. New paths in human cancer serology. *J. Exp. Med. 187:1163.*
4. Cormier, J. N., M. L. Salgaller, T. Prevette, K. C. Barracchini, L. Rivoltini, N. P. Restifo, S. A. Rosenberg, and F. M. Marincola. 1997. Enhancement of cellular immunity in melanoma patients immunized with a peptide from MART-1/Melan A. *Cancer J. Sci. Am. 3:37.*
5. Gajewski, T. F. 2000. Monitoring specific T-cell responses to melanoma vaccines: ELISPOT, tetramers and beyond. *Clin. Diagn. Lab. Immunol. 7:141.*
6. Kammula, U. S., F. M. Marincola, and S. A. Rosenberg. 2000. Real-time quantitative polymerase chain reaction assessment of immune reactivity in melanoma patients after tumor peptide vaccination. *J. Natl. Cancer Inst. 92:1336.*
7. Jager, E., S. Gnjatic, Y. Nagata, E. Stockert, D. Jager, J. Karbach, A. Neumann, J. Rieckenberg, Y.-T. Chen, G. Ritter, E. Hoffman, M. Arand, L. J. Old, and A. Knuth. 2000. Induction of primary NY-ESO-1 immunity: CD8$^+$ T lymphocyte and antibody responses in peptide-vaccinated patients with NY-ESO-1$^+$ cancers. *Proc. Natl. Acad. Sci. USA 97:12198.*
8. Marchand, M., N. van Baren, P. Weynants, V. Brichard, B. Dreno, M. H. Tessier, E. Rankin, G. Parmiani, F. Arienti, Y. Humblet, et al. 1999. Tumor regressions observed in patients with metastatic melanoma treated with an antigenic peptide encoded by gene *MAGE-3* and presented by HLA-A1. *Int. J. Cancer 80:219.*
9. Rosenberg, S. A., J. C. Yang, D. J. Schwartzentruber, P. Hwu, F. M. Marincola, S. L. Topalian, N. P. Restifo, M. Sznol, S. L. Schwarz, P. J. Spiess, et al. 1999. Impact of cytokine administration on the generation of anti-tumor reactivity in patients with metastatic melanoma receiving a peptide vaccine. *J. Immunol. 163: 1690.*
10. Mukherji, B., N. G. Chakraborty, S. Yamasaki, T. Okino, H. Yamase, J. R. Sporn, S. K. Kurtzman, M. T. Ergin, J. Ozols, J. Meehan, and F. Mauri. 1995. Induction of antigen-specific cytolytic T cells in situ in human melanoma by immunization with synthetic peptide-pulsed autologous antigen presenting cells. *Proc. Natl. Acad. Sci. USA 92:8078.*
11. Peiper, M., M. Nagoshi, D. Patel, J. A. Fletcher, P. S. Goegebuure, and T. J. Eberlein. 1997. Human pancreatic cancer cells (MPanc-96) recognized by autologous tumor-infiltrating lymphocytes after in vitro as well as in vivo tumor expansion. *Int. J. Cancer 71:993.*
12. Kammula, U. S., K.-H. Lee, A. Riker, E. Wang, G. A. Ohnmacht, S. A. Rosenberg, and F. M. Marincola. 1999. Functional analysis of antigen-specific T lymphocytes by serial measurement of gene expression in peripheral blood mononuclear cells and tumor specimens. *J. Immunol. 163:6867.*
13. Panelli, M. C., A. Riker, U. S. Kammula, K.-H. Lee, E. Wang, S. A. Rosenberg, and F. M. Marincola. 2000. Expansion of tumor/T cell pairs from fine needle aspirates (FNA) of melanoma metastases. *J. Immunol. 164:495.*
14. Dunbar, P. R., C. L. Smith, D. Chao, M. Salio, D. M. Shepherd, F. Mirza, M. Lipp, A. Lanzavecchia, F. Sallusto, A. Evans, et al. 2000. A shift in the phenotype of MelanA-specific CTL identifies melanoma patients with an active tumor-specific immune response. *J. Immunol. 165:6644.*
15. Nielsen, M.-B., V. Monsurro, S. Miguelse, E. Wang, A. Perez-Diez, K.-H. Lee, U. S. Kammula, S. A. Rosenberg, and F. M. Marincola. 2000. Status of activation of circulating vaccine-elicited CD8$^+$ T cells. *J. Immunol. 165:2287.*
16. Mukherji, B., and T. J. MacAlister. 1983. Clonal analysis of cytotoxic T cell response against human melanoma. *J. Exp. Med. 158:240.*
17. Cormier, J. N., M. L. Salgaller, T. Prevette, S. A. Rosenberg, and F. M. Marincola. 1996. Assessment of tumor specific immune response in patients receiving immunization with the MART-1 melanoma antigen immunodominant peptide. *Proc. Am. Assoc. Cancer Res. 37:476.*
18. Sznol, M., and F. M. Marincola. 2000. Principles of immune monitoring in cancer vaccine trials. In *Principles and Practice of the Biologic Therapy of Cancer.* 3rd Ed. S.A. Rosenberg, ed. Lippincott Williams & Wilkins, Philadelphia, p. 617.
19. Lee, K.-H., E. Wang, M.-B. Nielsen, J. Wunderlich, S. Migueles, M. Connors, S. M. Steinberg, S. A. Rosenberg, and F. M. Marincola. 1999. Increased vaccine-specific T cell frequency after peptide-based vaccination correlates with increased

susceptibility to in vitro stimulation but does not lead to tumor regression. *J. Immunol. 163:6292.*

20. Irvine, K. R., R. S. Chamberlain, E. P. Shulman, D. R. Surman, S. A. Rosenberg, and N. P. Restifo. 1997. Enhancing efficacy of recombinant anticancer vaccines with prime/boost regimens that use two different vectors. *J. Natl. Cancer Inst. 89:1595.*

21. Wang, M., V. Bronte, P. W. Chen, L. Gritz, D. Panicali, S. A. Rosenberg, and N. P. Restifo. 1995. Active immunotherapy of cancer with a nonreplicating recombinant fowl-pox virus encoding a model tumor-associated antigen. *J. Immunol. 154:4685.*

22. Nolan, G. P., S. Fiering, J. F. Nicolas, and L. A. Herzenberg. 1998. Fluorescence activated cell analysis and sorting of viable mammalian cells based on β-D-galactosidase activity after transduction of *Escherichia coli LacZ. Proc. Natl. Acad. Sci. USA 85:2603.*

23. Heid, C. A., J. Stevens, K. J. Livak, and P. M. Williams. 1996. Real time quantitative PCR. *Genome Res. 6:986.*

24. Prevost-Blondel, A., C. Zimmermann, C. Stemmer, P. Kulmburg, F. M. Rosenthal, and H. Pircher. 1998. Tumor-infiltrating lymphocytes exhibiting high ex vivo cytolytic activity fail to prevent murine melanoma tumor growth in vivo. *J. Immunol. 161:2187.*

25. Ochsenbein, A. F., P. Klenerman, U. Karrer, B. Ludewig, M. Pericin, H. Hengartner, and R. M. Zinkernagel. 1999. Immune surveillance against a solid tumor fails because of immunological ignorance. *Proc. Natl. Acad. Sci. USA 96:2233.*

26. Bellone, M., D. Cantarella, P. Castiglioni, M. C. Crosti, A. Ronchetti, M. Moro, M. P. Garancini, G. Casorati, and P. Dellabona. 2000. Relevance of the tumor antigen in the validation of three vaccination strategies for melanoma. *J. Immunol. 165:2651.*

27. Marincola, F. M., E. M. Jaffe, D. J. Hicklin, and S. Ferrone. 2000. Escape of human solid tumors from T cell recognition: molecular mechanisms and functional significance. *Adv. Immunol. 74:181.*

28. Wojtowicz-Praga, S. 1997. Reversal of tumor-induced immunosuppression: a new approach to cancer therapy. *J. Immunother. 20:165.*

29. Hahne, M., D. Rimoldi, M. Schroter, P. Romero, M. Schreier, L. E. French, P. Schneider, T. Bornand, A. Fontana, D. Lienard, et al. 1996. Melanoma cell expression of Fas (Apo-1/CD95) ligand: implications for tumor immune escape. *Science 274:1363.*

30. Ganss, R., and D. Hanahan. 1998. Tumor microenvironment can restrict the effectiveness of activated antitumor lymphocytes. *Cancer Res. 58:4673.*

31. Ashman, R. B. 1985. The influence of graft size on the induction of immunity versus tolerance to H-Y in H-2k strains of mice. *Immunogenetics 226:585.*

32. Chen, H. D., and W. K. Silvers. 1982. Studies on the behavior of H-Y incompatible skin grafts in rats. *J. Immunol. 128:2044.*

33. Prevost-Blondel, A., M. Neuenhahn, M. Rawiel, and H. Pircher. 2000. Differential requirement of perforin and IFN-γ in CD8 T cell-mediated immune responses against B16.F10 melanoma cells expressing a viral antigen. *Eur. J. Immunol. 30:2507.*

34. Campbell, I. L., A. Iscaro, and L. C. Harrison. 1988. IFN-γ and tumor necrosis factor-α: cytotoxicity to murine islets of Langerhans. *J. Immunol. 141:2325.*

35. Fried, M., R. O. Muga, A. O. Misore, and P. E. Duffy. 1998. Malaria elicit type 1 cytokines in the human placenta: IFN-γ and TNF-α associated with pregnancy outcomes. *J. Immunol. 160:2523.*

36. Geiger, K., E. Howes, M. Gallina, X. J. Huang, G. H. Travis, and N. Sarvetnick. 1994. Transgenic mice expressing IFN-γ in the retina develop inflammation of the eye and photoreceptor loss. *Invest Ophthalmol. Visual Sci. 35:2667.*

37. Guidotti, L. G., T. Ishikawa, M. V. Hobbs, B. Matzke, R. Schreiber, and F. V. Chisari. 1996. Intracellular inactivation of the hepatitis B virus by cytotoxic T lymphocytes. *Immunity 4:25.*

38. Rosenberg, S. A., J. C. Yang, D. Schwartzentruber, P. Hwu, F. M. Marincola, S. L. Topalian, N. P. Restifo, E. Dufour, L. Schwartzberg, P. Spiess, et al. 1998. Immunologic and therapeutic evaluation of a synthetic tumor associated peptide vaccine for the treatment of patients with metastatic melanoma. *Nat. Med. 4:321.*

39. Monsurro, V., M.-B. Nielsen, A. Perez-Diez, M. E. Dudley, E. Wang, S. A. Rosenberg, and F. M. Marincola. 2001. Kinetics of TCR use in response to repeated epitope-specific immunization. *J. Immunol. 166:5817.*